JOURNAL OF MAPS, 2015
http://dx.doi.org/10.1080/17445647.2015.1113391

SCIENCE

OPEN ACCESS

Mapping sediment–landform assemblages to constrain lacustrine sedimentation in a glacier-fed lake catchment in northwest Spitsbergen

Willem G.M. van der Bilt[a], Jostein Bakke[a] and Nicholas L. Balascio[b]

[a]Department of Earth Science and Bjerknes Centre for Climate Research, University of Bergen, Norway; [b]Lamont-Doherty Earth Observatory, Columbia University, New York, USA

ABSTRACT
Changes in the deposition of fine-grained rock-flour in glacier-fed lakes reflect glacier variability. This meltwater-driven signal is, however, often overprinted by other processes. To constrain the signature of lacustrine sedimentation, we mapped the catchment of glacier-fed Lake Hajeren in northwest Spitsbergen, identifying sediment sources and linking them to surface processes. To this end, we employed a combined approach of aerial image interpretation and field mapping. Our map comprises sediment–landform assemblages commonly found in pro-, peri- and paraglacial landsystems on Spitsbergen, including weathered moraines outboard Little Ice Age limits. Based on the presented map, we argue that mass-wasting does not directly impact lake sedimentation. Also, due to the scarcity of fines in historical glacial deposits, we suggest that modified glacigenic sediments only briefly affect a recorded glacier signal, following retreat. These findings highlight the value of geomorphological maps as tools to constrain catchment processes, improving the interpretation of lake sediment records.

ARTICLE HISTORY
Received 21 May 2015
Revised 14 October 2015
Accepted 24 October 2015

KEYWORDS
Spitsbergen; mapping; sediment transport; glacier-fed lake; paraglacial modification

1. Introduction

Glaciers are highly sensitive to climate change as demonstrated by their rapid retreat in response to current warming (WGMS, 1988–2011). Apart from geomorphological evidence, changes in glacier size are continuously recorded by variations in erosion rates and the flux of fine-grained (1–63 μm) minerogenic rock flour into distal glacier-fed lakes (Karlén, 1981; Leemann & Niessen, 1994). As such, sedimentary archives extracted from these lakes are widely used proxies of past climate variability (Bakke et al., 2010; Guyard, Chapron, St-Onge, & Labrie, 2013; McKay & Kaufman, 2009).

However, sedimentation in glacier-fed lakes is frequently affected by other sediment sources that leave a similar imprint in the lacustrine sediment record (Rubensdotter & Rosqvist, 2009; Vasskog et al., 2011). These commonly include reworked glacigenic sediments that have been modified by non-glacial processes (Ballantyne, 2002; Dahl, Bakke, Lie, & Nesje, 2003). In addition to such paraglacial modification (Church & Ryder, 1972), mass-wasting can overprint the signature of a glacier signal (Vasskog et al., 2011). The impact of these processes should be understood to ensure an accurate reconstruction of a glacier variability (Jansson, Rosqvist, & Schneider, 2005; Rubensdotter & Rosqvist, 2009).

Here, we present a 1:8000 scale geomorphological map of the glaciarized catchment of lake Hajeren in northwest Spitsbergen (79°15’N: 11°31’E) (Figures 1 and 2), based on aerial photographs and ground-truthing. Mapping enables us to identify sediment sources and transport mechanisms that may affect the lacustrine sediment record (Carrivick & Tweed, 2013). We aim to assess the relationship between the morphology of mapped landforms and their genesis to gain a process-based understanding of sediment transport in the catchment. This information will help validate the robustness of a separately published glacier activity reconstruction, based on sediments from Lake Hajeren (van der Bilt et al., 2015).

2. Study site

The 2.96 km^2 Hajeren watershed, mapped for this study, is located on the Mitra peninsula in northwest Spitsbergen (79°15’N: 11°31’E) (Figures 1 and 2). The catchment is unvegetated and covered by unconsolidated sediments and Grenvillian age schist bedrock belonging to the Signehamna formation (Ohta et al., 2002). The mean annual air temperature is approximately −5°C (Førland, Benestad, Hanssen-Bauer, Haugen, & Skaugen, 2011) and the area falls within the zone of continuous permafrost (Nelson, Anisimov, & Shiklomanov, 2002). At present, two small glaciers occupy cirques in the Southeast sector of the Hajeren catchment, the North Glacier (0.08

CONTACT Willem G.M. van der Bilt willemvanderbilt@gmail.com, willemvanderbilt@uib.no

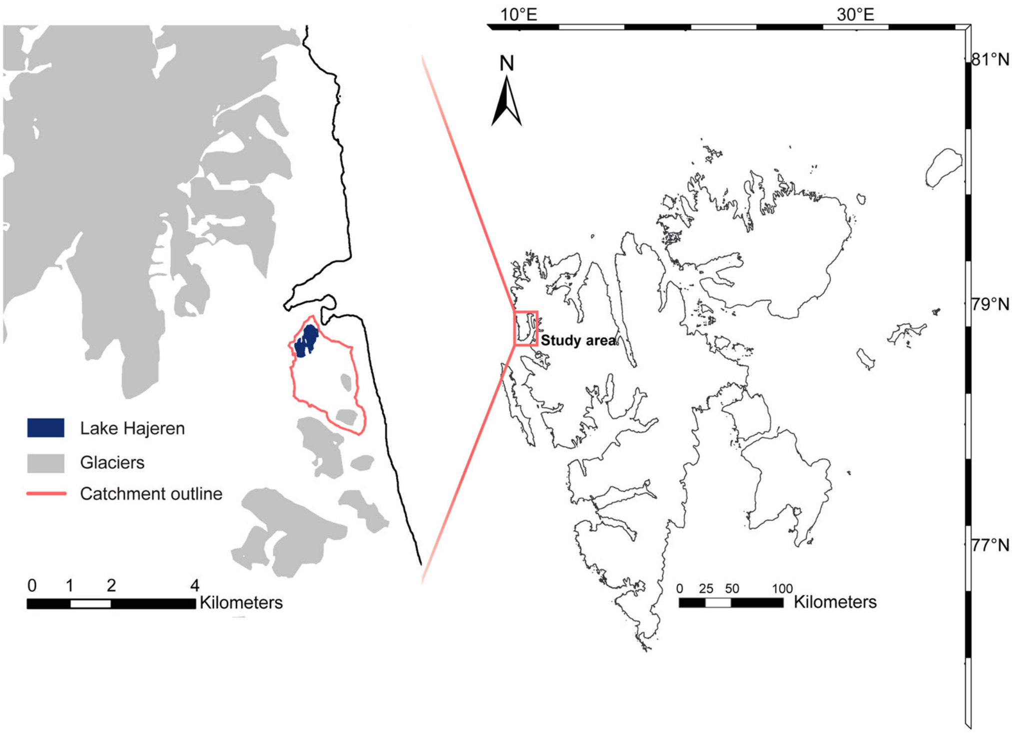

Figure 1. Map showing the Svalbard archipelago and an inset of the study area in the Hajeren catchment. Lake Hajeren is indicated in blue in the left panel, while present-day glacier extent is shown in grey (NPI, 2015).

km^2) and South Glacier (0.17 km^2). Both glaciers drain into Lake Hajeren in the northwest sector of the catchment. Aerial photographs show the glaciers of the Hajeren catchment reached a historical maximum during the early twentieth century culmination of the Little Ice Age (LIA) (Norwegian Polar Institute [NPI], 1936), like most Svalbard glaciers (Glasser & Hambrey, 2014; Hagen, Melvold, Pinglot, & Dowdeswell, 2003; Salvigsen & Høgvard, 2006). Also, documented front positions show that the North and South glaciers have subsequently been retreating (NPI, 2015).

3. Map compilation

3.1. Mapping methods

The presented map was compiled using a combination of aerial image interpretation and field mapping. The former was carried out using a 195.8 megapixel aerial photograph from the NPI with a 40–50 cm ground sampling distance, taken with a Microsoft Vexcel UltraCam-Xp in July 2009 (NPI, 2009). This image was provided in a digital.tiff format and was neither ortho- nor georectified. Also, the image was not supplied with a set of Rational Polynomial Coefficients

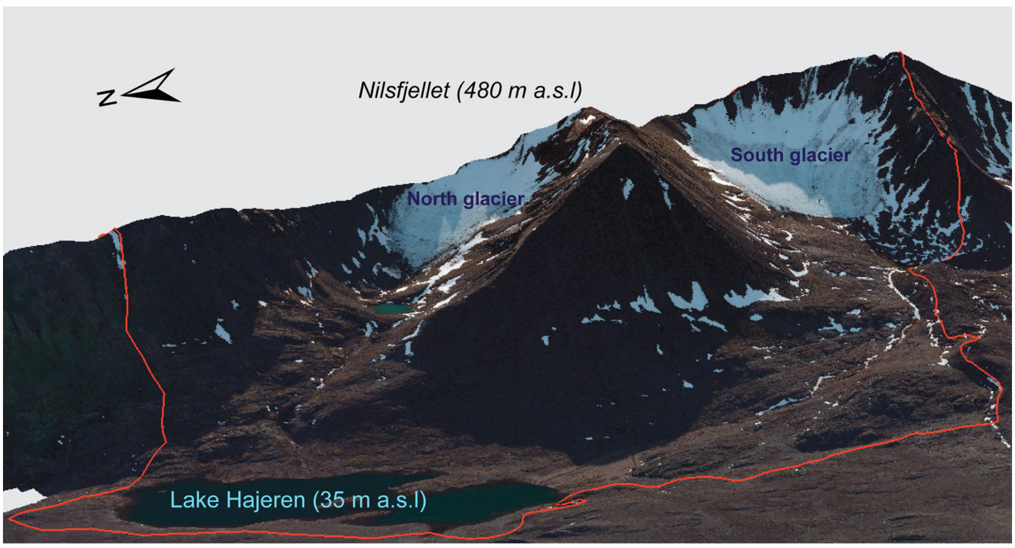

Figure 2. Oblique view of the Hajeren catchment toward the west (NPI, 2009, 2013). North as well as South glaciers are indicated and the catchment outline is delineated by a red line.

(RPCs) and could therefore not be readily orthorectified (Faste Aas, personal communication). Instead, to put the file into a known coordinate system, it was georeferenced, establishing tie-points with geographical information system (GIS) data of the 2009 outline of lakes and glaciers as well as a 20 m Digital Elevation Model (DEM), all provided by the NPI (|NPI, 2013, 2014). This projection was later verified against field-logged Ground Control Points (GCP), recorded with a handheld Global Positioning System (GPS) receiver at easily identifiable features.

The 2009 aerial photograph was georectified using Esri ArcMap 10.2, applying a first-order polynomial transformation. To this end, we selected 18 control points on polygons of Lake Hajeren and both North and South Glaciers from 2009 (NPI, 2014), projected to universal transverse Mercator (UTM) zone 33N on the WGS84 ellipsoid.

Next, to correct for distortion caused by catchment relief, we selected additional summit control points on a 20 m resolution DEM of Svalbard. We then draped the rectified aerial photograph over the 20 m DEM in ArcScene 10.2 to highlight topographic features (Figure 2). We subsequently used this visualization for a preliminary survey of the sediment cascade between glaciers and lake, identifying sediment sources that may affect the lacustrine sediment record.

Mapping was mostly carried out during a 2-day field survey on 5 and 6 September 2014. As the study area falls outside existing differential GPS (DGPS) networks, we used a regular Garmin GPSMAP 62S with an indicated 5 m accuracy. Even though the outlined pre-fieldwork survey enabled us to target our field effort, some sections could not be mapped on site. These comprise high-lying steep terrain above 250 m a.s.l., either covered by bedrock, weathered material, the upper reaches of talus cones or glacier ice. These easily identifiable units were mapped using the discussed georectified 2009 aerial photograph. As outlined, this visualization was ground-truthed prior to mapping, using GPS-logged GCPs of mapped and photographed features (Figure 4). Based on the correspondence between these datasets, we argue that geocorrection errors fall within the measurement uncertainty of the GPS device.

3.2. Map production

The presented map was produced in Esri ArcMap 10.2 and Adobe Illustrator CS6. First, GPS tracks and waypoints of field-logged landforms were imported, converting the former to points and the latter to polylines or polygons. Information on glacier and lake extent was taken from an NPI GIS database (NPI, 2014). To delineate the Hajeren catchment, we applied the hydrology toolset in the ArcGIS 10.2. Aerial-mapped landforms were traced using heads-up digitization. For this purpose, shadowed sections of the image were first processed using the shadows and highlights adjustment in Adobe Photoshop CS6. To warrant compatibility with other regional maps, features were drawn following the standardized symbology of the Geological Survey of Norway (NGU) (Bergstrøm, Reite, Sveian, & Olsen, 2001). In the text, we occasionally deviate from this generalized scheme to provide more specific morphological details. The ensuing map was displayed on an A3 format data frame and overlain by a 100m kilometer-rounded UTM grid, using a 1:8000 reference scale and then exported to Adobe illustrator CS6 for formatting.

4. Mapped sediment–landform assemblages

In total, we identified 29 separate landforms and features on the presented map (Main Map). The catchment is dominated by expanses of highly weathered material, concentrated around Lake Hajeren. These often appear modified by periglacial processes as demonstrated by the presence of polygonal ground, solifluction lobes and frost-shattered surfaces. Glacier forelands are predominantly covered by tills and (marginal) moraine deposits with frequent occurrences of large boulders and kettle holes. Fan-shaped mass movement deposits are located on the steeper mountain sides and often associated with rock glaciers. Glaciofluvial deposits are found in forelands and valley floors as floodplains (Sandurs). Lacustrine deposits are concentrated around Lake Hajeren as well as a small lake found in front of the North glacier. Catchment hydrology, which plays a vital role in sediment transport, as well as weathered surfaces and exposed bedrock surfaces are also indicated on the map. Following Evans, Twigg, and Orton (2010), we categorized the surficial geology of the catchment into sediment–landform assemblages to allow discussion of their genesis and their role in the catchment sediment cascade (Paragraph 5).

4.1. Till and moraines

Marginal moraines are found in front of both North and South glaciers and were categorized into Stage 1 and Stage 2 deposits. However, stage 1 deposits were solely observed at the North Glacier and Stage 2 deposits are most prominent here (Figure 3).

4.1.1. North Glacier

Stage 1 moraines were deposited as a complex of mounds. In total, we discerned 12 westward facing 10–20 m high mounds, mainly comprising boulders (Figure 3). Extensive frost-shattering and lichen-coverage indicates heavy weathering. The most distal of these lies approximately 140 m in front of Stage 2 deposits. Also, both deposits intersect at around 177

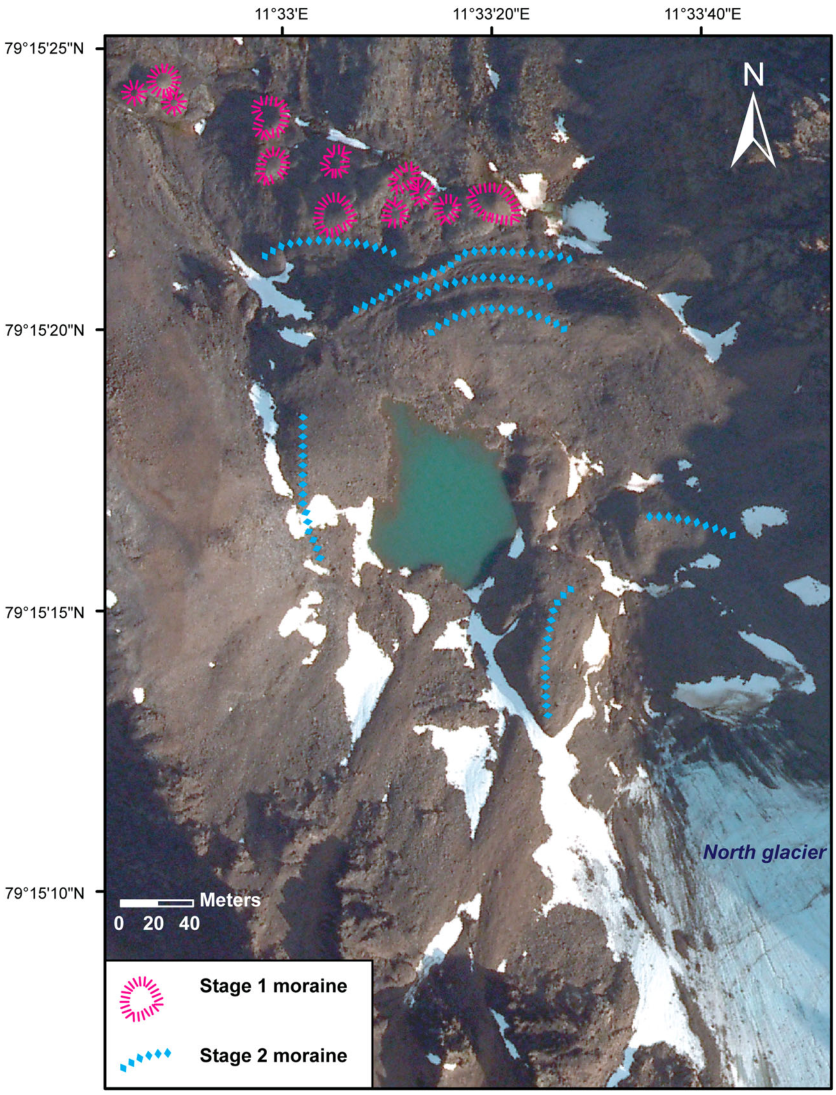

Figure 3. A close-up of the foreland of the North glacier, showing the discussed Stage 1 and 2 moraine deposits, with an aerial image in the background (NPI, 2009).

m a.s.l. (Figure 4(a)). Stage 2 moraines in front of the North glacier comprise a moraine-mound complex (Glasser & Hambrey, 2014; Hambrey, Huddart, Bennett, & Glasser, 1997), consisting of marginal composite ridges that are transversely aligned with the glacier front and not uniformly pronounced. The outer 50 m of the system is characterized by small-scale ridges with ± 1 m high crests (Figure 4(b)). The inner part is composed of 3 large-scale 40 m high ridges that are strewn with frequent large boulders. The gravelly material of the innermost ridge is draped with silt and appears recently exposed. Fresh deposits, inside the North Glacier's Stage 2 moraines, comprise a series of near conical mounds, oriented parallel to the glacier front. Based on large amounts of supraglacial debris in combination with abundant unconsolidated material and the presence of kettle holes, we interpret these as ice-cored moraines (mapped as 'till'). Finally, a pair of fairly symmetrical rounded ridges is identified along both sides of the glacier. These are interpreted as lateral moraines, smoothed by material delivered from the slopes surrounding the glacier.

4.1.2. South glacier

The foreland of the South Glacier is delineated by an undulating boulder-strewn Stage 2 moraine ridge (Figure 4(c)). Additionally, a pronounced 30 m high lateral moraine flanks the South side of the glacier. A ridge of bouldery diamict, interpreted as a frontal moraine, nudges the massive lateral moraine complex of adjacent Karlbreen. The foreland itself is covered by ± 2 m high mounds of bouldery diamict. Based on the high concentration of supraglacial debris on the glacier front, we suggest these are ablation moraines, following the definition of Bennett and Glasser (2009). In general, moraines outside of the present South glacier are much less pronounced than those seen at the North Glacier (Figure 4(c)).

4.2. Lacustrine deposits

In the field, old lake shorelines, marked by sets of pebbly pavement features, were identified ± 1.5 m above contemporary water level at Hajeren. These run parallel to the present-day shore and can be discerned

Figure 4. Field pictures of (a) the contact between Stage 1(blue) and 2 (red) deposits at the North glaciers (facing east), (b) composite ridges on Stage 2 moraines in front of the North glacier (facing North), (c) Stage 2 moraines of the South glacier (view toward the northwest), (d) ice-contact lake fronting the North glaciers with exposed shorelines indicated by the yellow dashed line (facing south), (e) snow-covered rock glacier termini and associated talus fans (view toward the northeast) and (f) in-active outwash plain draining the North Glacier (facing east).

around most of the lake's perimeter. Their presence is accentuated by visible differences in vegetation cover and the degree of weathering. Areas between the former and present shoreline were mapped as lacustrine deposits. Along the southwest of Lake Hajeren, we mapped a bouldery spillway that drains the lake. The elevation of this presently dry outlet corresponds to that of the set of old shorelines. Finally, a 600 m^2 pro-glacial lake sits between the North Glacier and its Stage 2 moraines (Figure 4(d)). Based on the interpretation of the surrounding terrain as ice-cored deposits, this lake is described as an ice-contact lake after Ashley (1995). Silt-draped exposed shorelines suggest a recent drop in water level.

4.3. Periglacial features

Large swaths of mapped weathered surfaces in the Hajeren catchment are covered by periglacial features, mostly patterned ground (Main Map). These predominantly consist of contiguous sorted polygons with an average diameter of ± 1 m. Frost-shattering of weathered bouldery deposits is mainly restricted to deposits of former (in-active) meltwater channels (c.f. '4.5 glaciofluvial deposits'). Solifluction lobes are restricted to a moderately gentle (16.5°) exposed southwest facing slope in the southern part of the watershed. Here, 10–30 m wide lobes group together in sheets along a stepped profile on the vegetated soil that characterize the area. We also classify the rock glaciers of the Hajeren watershed as periglacial features due to their previously acknowledged association with upslope colluvium (Barsch, 1977; Johnson, 1974). Rock glaciers in the Hajeren catchment share a set of morphological characteristics. Fronts terminate around the 225 m contour line, are approximately 15 m high and originate from individual talus cones (Figure 4(e)). As such, only termini are mapped as rock glaciers. Moreover, all termini were snow covered both on aerial photographs and in the field (Figure 4(e)). Judging by steep snouts and unvegetated unstable surfaces, we assume that these rock glaciers are active (Martin & Whalley, 1987). This is also supported by the fact that the mapped area falls well within the zone of continuous permafrost (Nelson et al., 2002). Surface material is dominated by open angular boulder-sized debris, while snow is concentrated in voids (Martin & Whalley, 1987). Finally, all mapped rock glaciers have a south-westerly aspect to the leeside of prevailing easterly winds (Beine, Argentini, Maurizi, Mastrantonio, & Viola, 2001).

4.4. Slope deposits

The stratigraphy of slope deposits could not be investigated in full detail during our field survey. Hence, we were not able to distinguish between processes of downslope wasting with certainty and grouped these deposits on our map as mass movement deposits. Slope deposits are mostly found below steep rock fall areas where periglacial processes such as frost wedging may detach bedrock. Here, colluvium accumulates near the rock fall shadow and mantles concave slopes in lobate-shaped talus sheets. All mapped fans terminate far from the shores of Lake Hajeren (Main Map). Often, these fans comprise fining upward sequences with a downslope concentration of large boulders known as out-runners (Blikra & Nemec, 1998). In general, the surface of slope deposits appears fresh compared to surrounding deposits, suggesting regular activation. This notion is supported by the previously mentioned large supply of supraglacial debris as both glaciers are flanked by colluvial fans. Based on their consistent co-occurrence (Figure 4(e)), we suggest that talus cones extend into downslope rock glaciers following Ballantyne (2002).

4.5. Glaciofluvial deposits

In the Hajeren catchment, glaciofluvial deposits are concentrated in the foreland of the South Glacier and on the valley floor. At both glaciers, these glacial and pro-glacial systems are connected by high-gradient channels that cross the steep terrain between cirques and valley floor. Here, meltwater has carved 20 m deep ravines into the erosive marble found in the upper part of the catchment (> 140 m a.s.l.). Moreover, the channel coming from the South Glacier has cut a glaciofluvial scarp into the moraine complex of Karlbreen, bordering the Hajeren watershed to the west. At the South Glacier, outwash emerges from a single supraglacial channel that has incised a laterally constrained (± 30 m wide) ice-proximal fan into the adjacent till deposits. In contrast, no outwash emerges in the foreland of the North Glacier. From both cirques, Sandurs radiate out onto the valley floor toward the shores of Lake Hajeren. The southernmost plain is particularly extensive, with a width of 130 m at its distal end. Up-valley, it develops into a valley Sandur, hemmed in by mountainsides. Cross-cutting relations are apparent at its southern edge, where fluvial erosion has cut into severely frost-shattered weathered deposits with traces of currently inactive meltwater channels. Similar channel deposits are found adjacent to the previously discussed Stage 1 mounds in front of the North Glacier. The gently sloping surface (2.75°) of the southern Sandur is covered by an alternation of gravelly bars and both active as well as inactive pebbly braided meltwater channels. The Sandur in the northern part of the catchment is smaller and characterized by coarser material (pebbles-boulders), suggesting a high energy level during deposition. Active meltwater channels appear over-dimensioned in relation to present flow. This is also attested by a minor inactive outwash plain that branches off from the main Sandur (Figure 4(f)). These deposits are frost-shattered and lichen-covered, indicating prolonged inactivity (Figure 4(f)).

5. Discussion

Following the identification of sediment–landform assemblages, we use the ensuing geomorphological (Main Map) to assess sediment delivery to Lake Hajeren. As previously stressed, a process-based understanding of landforms is critical to understand the signature of lacustrine sedimentation in glacier-fed sites (Carrivick & Tweed, 2013; Dahl et al., 2003). In the case of Lake Hajeren, this insight will help evaluate the robustness of the separately published glacier activity reconstruction, based on the lacustrine sediment record (van der Bilt et al., 2015).

The observed difference in the degree of weathering between Stage 1 and Stage 2 moraines suggests that glacial erosion has repeatedly affected sedimentation in the catchment. Based on the discussed 1936 aerial photograph (NPI, 1936), as well as a similar relation to present ice extent as nearby glacier systems (Evans, Strzelecki, Milledge, & Orton, 2012; Hambrey et al., 2005; Hodson et al., 1998; Røthe et al., 2015), Stage 2 moraines are assumed to have been deposited during the LIA Although chronological control is lacking, a high degree of weathering and deposition outside of Stage 2 deposits indicates that Stage 1 moraines at the North Glacier represent a Holocene glacier maximum that predates the LIA. Based on a minimum age of 6.7 ka BP for an ice-cored moraine fronting adjacent Karlbreen (Røthe et al., 2015), we propose an Early Holocene age.

The combination of composite ridges and ice-cored moraines, observed at Stage 2 deposits fronting the North Glacier, often indicate glacial deformation of permafrozen material on Svalbard (Boulton, Van der Meer, Beets, Hart, & Ruegg, 1999; Etzelmüller &

Hagen, 2005). Based on this landsystem signature, we infer erosive polythermal basal conditions for the North Glacier with temperate ice and a frozen snout as described for Spitsbergen glaciers (e.g. Evans et al., 2012; Hambrey et al., 2005). The observed composite ridges are grouped in small- and large-scale features. We suggest that the former are the result of seasonal glacier fluctuations whereas the latter reflect persistent glacier advances following Bennett and Glasser (2009). Based on the dominance of supraglacial meltwater drainage (Hodson et al., 1998) and a lack of glacigenic sediments (Fitzsimons, 2003), we tentatively infer a non-erosive cold-based regime for the South Glacier. Though geomorphological evidence is lacking, we cannot exclude the possibility of a regime shift due to recent thinning as reported by Björnsson et al. (1996). To conclude, we argue that only the North Glacier is capable of producing significant amounts of glacigenic sediments through glacial erosion.

Large areas of the catchment were mapped as periglacial deposits, mainly comprising patterned ground, particularly around Lake Hajeren. Patterned ground exclusively consists of polygonal ground, suggesting formation by lateral squeezing and confinement of rock material as suggested by Kessler and Werner (2003). In contrast, more dynamic periglacial features (i.e. solifluction lobes and rock glaciers) are concentrated in steeper sections of the catchment, particularly on the forelands of both glaciers (Main Map). The same is true for associated slope deposits (paragraph 4.4). We argue that the combination of comparatively stable features around the lake and dynamic deposits in steeper sections shields the lacustrine record against mass-wasting processes.

Our map demonstrates that glacifluvial drainage couples glacial, pro-glacial and lacustrine environments in the catchment. We therefore argue that glaciofluvial transport is the dominant sediment delivery pathway to Lake Hajeren. In addition to the transfer of glacial and pro-glacial sediments, streams also act as agents of erosion, cutting through bedrock in the steep transition between foreland and Sandur of the North Glacier`s debris cascade (Benn & Evans, 2014).

Moreover, meltwater streams rework older glacigenic deposits in the catchment. Near the South Glacier, for example, meltwater incises diamict deposits. The potential for paraglacial reworking is particularly great for the fresh (post)-LIA sediments stored in the Stage 2 foreland of the erosive North Glacier. However, fine-grained reworked deposits, which may leave a similar imprint on the lacustrine sediment record as fresh glacial flour (Jansson et al., 2005; Rubensdotter & Rosqvist, 2009), are scarce in the catchment (paragraph 4.1). As both glaciers were more active in the recent past (NPI, 1936), this observation favors a rapid exhaustion of fine-grained glacigenic sources, in line with the findings of Harbor and Warburton (1993) for similar small catchments. Still, we cannot rule out that postglacial processes, like melt-out of the ice-cored moraines near the North Glacier, may remobilize glacigenic sediments over longer timescales as suggested by Etzelmüller and Hagen (2005). However, following Leonard (1997), we argue that the sediment record of Lake Hajeren is mainly affected by paraglacial modification during transition phases subsequent to retreat or advance.

The observed presence of inactive and over-sized meltwater channels and Sandur sections, in combination with raised old lake shorelines, is indicative of past hydrological change. Previous monitoring studies in glaciarized catchments have demonstrated a strong correlation between glacier melt and run-off (Leemann & Niessen, 1994; Liermann, Beylich, & van Welden, 2012). Based on the large degree of past glacier activity, indicated by Stage 1 and 2 moraines, we tentatively attribute these inferred episodic discharge changes to glacier variability. Nevertheless, we cannot exclude the possibility that these features result from channel migration as suggested by Williams and Rust (1969), redepositing glacifluvial material in the process. Moreover, fill/drain cycles of ephemeral lakes similar to the ice-contact lake fronting the North glacier may have contributed to run-off pulses, in addition to trapping glacial flour (Carrivick & Tweed, 2013).

6. Conclusions

The presented map enables us to gain a process-based understanding of sedimentation in the Hajeren catchment. This, in turn, helps constrain the impact of mass-wasting and paraglacial modification on the lacustrine sediment record, validating the findings of van der Bilt et al. (2015). In summary, we identify glaciofluvial transport as the dominant sediment delivery pathway in the catchment, coupling lake Hajeren and the catchment's main depositional zones in the forelands of North and South glaciers. Most observed landform assemblages are solely found in these areas, as shown on our map (Main Map). In contrast, the area around Lake Hajeren is covered by gently sloping expanses of weathered material, minimizing the impact of mass-wasting on the lacustrine sediment record. Based on its discussed land system signature, we claim that the North Glacier is the dominant producer of glacigenic sediments in the catchment. However, due to an observed lack of fines, we propose a short paraglacial period, characteristic for comparable small catchments (Harbor & Warburton, 1993). Following Leonard (1997), we argue that paraglacial modification only affects the lacustrine record briefly after glacier retreat or advance. In conclusion, this study underlines the value of geomorphological mapping as a tool to constrain lacustrine sedimentation. Similar exercises could therefore contribute to the robustness of attendant lake sediment studies.

Software

Mapping was carried out using Esri ArcMap 10.2. In addition to the editor, we used both georeferencing and spatial analyst toolbars. The resulting map was edited using Adobe illustrator CS6.

Acknowledgments

We would like to thank Raymond Bradley, William D'Andrea, Greg de Wet, Sædís Ólafsdóttir, Marthe Gjerde and Torgeir Røthe for their assistance in the field. WGMB would like to express his gratitude for Harald Faste Aas at the NPI for providing aerial photographs of the study area. Finally, we thank our reviewers, Peter Jansson, Matti Peljo and Martin Geilhausen, for greatly improving this manuscript.

Disclosure statement

No potential conflict of interest was reported by the authors.

Funding

This study has received funding from the Norwegian Research Council through the project «Shifting Climate States of the Polar Regions» (210004). This work was also supported by the Norwegian Research Council Arctic Field Grant, awarded to WGMB, NLB and JB.

ORCID

Willem G.M. van der Bilt http://orcid.org/0000-0003-3157-451X

References

Ashley, G. (1995). Glaciolacustrine environments. *Glacial Environments*, *1*, 417–444.

Bakke, J., Dahl, S. O., Paasche, Ø., Riis Simonsen, J., Kvisvik, B., Bakke, K., & Nesje, A. (2010). A complete record of Holocene glacier variability at Austre Okstindbreen, northern Norway: An integrated approach. *Quaternary Science Reviews*, *29*(9), 1246–1262.

Ballantyne, C. K. (2002). Paraglacial geomorphology. *Quaternary Science Reviews*, *21*(18), 1935–2017.

Barsch, D. (1977). Nature and importance of mass-wasting by rock glaciers in alpine permafrost environments. *Earth Surface Processes*, *2*(2–3), 231–245.

Beine, H., Argentini, S., Maurizi, A., Mastrantonio, G., & Viola, A. (2001). The local wind field at Ny-Å lesund and the Zeppelin mountain at Svalbard. *Meteorology and Atmospheric Physics*, *78*(1–2), 107–113.

Benn, D., & Evans, D. J. (2014). *Glaciers and glaciation*. New York: Routledge.

Bennett, M. M., & Glasser, N. F. (2009). *Glacial geology: Ice sheets and landforms*. Chichester: John Wiley & Sons.

Bergstrøm, B., Reite, A., Sveian, H., & Olsen, L. (2001). Feltrutiner, kartleggingsprinsipper og standarder for kvartærgeologisk kartlegging-løsmassekartlegging ved NGU. *Norges geologiske undersokelse Internal Report 2001.018*.

van der Bilt, W. G. M., Bakke, J., Vasskog, K., D'Andrea, W. J., Bradley, R. S., & Ólafsdóttir, S. (2015). Reconstruction of glacier variability from lake sediments reveals dynamic Holocene climate in Svalbard. *Quaternary Science Reviews*, *126*, 201–218. doi: http://dx.doi.org/10.1016/j.quascirev.2015.09.003

Björnsson, H., Gjessing, Y., Hamran, S.-E., Hagen, J. O., Liestøl, O., Pálsson, F., & Erlingsson, B. (1996). The thermal regime of sub-polar glaciers mapped by multi-frequency radio-echo sounding. *Journal of Glaciology*, *42* (140), 23–32.

Blikra, L. H., & Nemec, W. (1998). Postglacial colluvium in western Norway: Depositional processes, facies and palaeoclimatic record. *Sedimentology*, *45*(5), 909–959.

Boulton, G., Van der Meer, J., Beets, D., Hart, J., & Ruegg, G. (1999). The sedimentary and structural evolution of a recent push moraine complex: Holmstrømbreen, Spitsbergen. *Quaternary Science Reviews*, *18*(3), 339–371.

Carrivick, J. L., & Tweed, F. S. (2013). Proglacial lakes: Character, behaviour and geological importance. *Quaternary Science Reviews*, *78*(0), 34–52. doi: 10.1016/j.quascirev.2013.07.028

Church, M., & Ryder, J. M. (1972). Paraglacial sedimentation: A consideration of fluvial processes conditioned by glaciation. *Geological Society of America Bulletin*, *83* (10), 3059–3072.

Dahl, S. O., Bakke, J., Lie, Ø., & Nesje, A. (2003). Reconstruction of former glacier equilibrium-line altitudes based on proglacial sites: An evaluation of approaches and selection of sites. *Quaternary Science Reviews*, *22*(2), 275–287.

Etzelmüller, B., & Hagen, J. O. (2005). Glacier-permafrost interaction in Arctic and alpine mountain environments with examples from southern Norway and Svalbard. *Geological Society, London, Special Publications*, *242*(1), 11–27.

Evans, D. J. A., Strzelecki, M., Milledge, D. G., & Orton, C. (2012). Hørbyebreen polythermal glacial landsystem, Svalbard. *Journal of Maps*, *8*(2), 146–156. doi:10.1080/17445647.2012.680776

Evans, D. J. A., Twigg, D. R., & Orton, C. (2010). Satujökull glacial landsystem, Iceland. *Journal of Maps*, *6*(1), 639–650. doi:10.4113/jom.2010.1129

Fitzsimons, S. J. (2003). Ice-marginal terrestrial landsystems: Polar continental glacier margins. *Glacial Landsystems. Arnold, London*, *5*, 89–110.

Førland, E. J., Benestad, R., Hanssen-Bauer, I., Haugen, J. E., & Skaugen, T. E. (2011). Temperature and precipitation development at Svalbard 1900–2100. *Advances in Meteorology, 2011*, 1–14.

Glasser, N., & Hambrey, M. J. (2014). Ice-marginal terrestrial landsystems: Svalbard polythermal glaciers. In D. Evans (Ed.), *Glacial landsystems* (pp. 65–87). Florence, KY: Taylor & Francis.

Guyard, H., Chapron, E., St-Onge, G., & Labrie, J. (2013). Late-Holocene NAO and ocean forcing on high-altitude proglacial sedimentation (Lake Bramant, Western French Alps). *The Holocene*, *23*, 1163–1172.

Hagen, J. O., Melvold, K., Pinglot, F., & Dowdeswell, J. A. (2003). On the net mass balance of the glaciers and ice caps in Svalbard, Norwegian Arctic. *Arctic, Antarctic, and Alpine Research*, *35*(2), 264–270.

Hambrey, M. J., Huddart, D., Bennett, M. M., & Glasser, N. F. (1997). Genesis of 'hummocky moraines' by thrusting in glacier ice: Evidence from Svalbard and Britain. *Journal of the Geological Society*, *154*(4), 623–632.

Hambrey, M. J., Murray, T., Glasser, N. F., Hubbard, A., Hubbard, B., Stuart, G., … Kohler, J. (2005). Structure and changing dynamics of a polythermal valley glacier on a centennial timescale: Midre Lovénbreen, Svalbard. *Journal of Geophysical Research: Earth Surface (2003–2012)*, *110*(F1), 1–19.

Harbor, J., & Warburton, J. (1993). Relative rates of glacial and nonglacial erosion in alpine environments. *Arctic and Alpine Research*, *25*, 1–7.

Hodson, A., Gurnell, A., Tranter, M., Bogen, J., Hagen, J. O., & Clark, M. (1998). Suspended sediment yield and transfer processes in a small High-Arctic glacier basin, Svalbard. *Hydrological Processes*, *12*(1), 73–86.

Jansson, P., Rosqvist, G., & Schneider, T. (2005). Glacier fluctuations, suspended sediment flux and glacio-lacustrine sediments. *Geografiska Annaler: Series A, Physical Geography*, *87*(1), 37–50.

Johnson, P. G. (1974). Mass movement of ablation complexes and their relationship to rock glaciers. *Geografiska Annaler. Series A. Physical Geography*, *56*, 93–101.

Karlén, W. (1981). Lacustrine sediment studies. A technique to obtain a continuous record of Holocene glacier variations. *Geografiska Annaler. Series A. Physical Geography*, *63*, 273–281.

Kessler, M., & Werner, B. (2003). Self-organization of sorted patterned ground. *Science*, *299*(5605), 380–383.

Leemann, A., & Niessen, F. (1994). Varve formation and the climatic record in an Alpine proglacial Lake: Calibrating annually-laminated sediments against hydrological and meteorological data. *The Holocene*, *4*(1), 1–8.

Leonard, E. M. (1997). The relationship between glacial activity and sediment production: Evidence from a 4450-year varve record of neoglacial sedimentation in Hector Lake, Alberta, Canada. *Journal of Paleolimnology*, *17*(3), 321–332.

Liermann, S., Beylich, A. A., & van Welden, A. (2012). Contemporary suspended sediment transfer and accumulation processes in the small proglacial Sætrevatnet subcatchment, Bødalen, western Norway. *Geomorphology*, *167-168*(0), 91–101. doi:10.1016/j.geomorph.2012.03.035

Martin, H. E., & Whalley, W. B. (1987). Rock glaciers part 1: Rock glacier morphology: Classification and distribution. *Progress in Physical Geography*, *11*(2), 260–282.

McKay, N. P., & Kaufman, D. S. (2009). Holocene climate and glacier variability at Hallet and Greyling Lakes, Chugach Mountains, south-central Alaska. *Journal of Paleolimnology*, *41*(1), 143–159.

Nelson, F., Anisimov, O., & Shiklomanov, N. I. (2002). Climate change and hazard zonation in the circum-Arctic permafrost regions. *Natural Hazards*, *26*(3), 203–225.

NPI. (1936). s36_2066. In s. dpi (Ed.). Svalbard: NPI.

NPI. (2009). Aerial photograph, ID: 13822/730. In 13822 (Ed.), (Vol. 310 mb): Norwegian Polar Institute

NPI. (2013). *S100 terrengmodell Svalbard 20*20 m.*

NPI (Cartographer). (2014). Kartdata Svalbard 1:100 000 (S100 Kartdata).

NPI. (2015). Svalbardkartet. 2014, from www.npolar.no/svalbardkartet

Ohta, Y., Larionov, A. N., Tebenkov, A. M., Lepvrier, C., Maluski, H., & Lange, M., & Hellebrandt, B. (2002). Single-zircon Pb-evaporation and 40Ar/39Ar dating of the metamorphic and granitic rocks in north-west Spitsbergen. *Polar Research*, *21*(1), 73–89.

Røthe, T. O., Bakke, J., Vasskog, K., Gjerde, M., D'Andrea, W. J., & Bradley, R. S. (2015). Arctic Holocene glacier fluctuations reconstructed from lake sediments at Mitrahalvøya, Spitsbergen. *Quaternary Science Reviews*, *109*(0), 111–125. doi:10.1016/j.quascirev.2014.11.017

Rubensdotter, L., & Rosqvist, G. (2009). Influence of geomorphological setting, fluvial-, glaciofluvial-and mass-movement processes on sedimentation in alpine lakes. *The Holocene*, *19*(4), 665–678.

Salvigsen, O., & Høgvard, K. (2006). Glacial history, Holocene shoreline displacement and palaeoclimate based on radiocarbon ages in the area of Bockfjorden, north-western Spitsbergen, Svalbard. *Polar Research*, *25*(1), 15–24.

Vasskog, K., Nesje, A., Støren, E. N., Waldmann, N., Chapron, E., & Ariztegui, D. (2011). A Holocene record of snow-avalanche and flood activity reconstructed from a lacustrine sedimentary sequence in Oldevatnet, western Norway. *The Holocene*, *21*, 597–614.

WGMS. (1988–2011). Glacier Mass Balance Bulletin (GMBB). Retrieved September 25, 2014, from http://www.wgms.ch/gmbb.html

Williams, P. F., & Rust, B. R. (1969). The sedimentology of a braided river. *Journal of Sedimentary Research*, *39*(2), 649–679.